Magnetic Resonance Imaging of Fe_3O_4 Nanoparticles Embedded in Living Magnetotactic Bacteria for Potential Use as Carriers for *In Vivo* Applications

Ouajdi Felfoul, S*tudent Member IEEE,* Mahmood Mohammadi and, Sylvain Martel*, *Senior Member IEEE*

NanoRobotics Laboratory, Department of Computer Engineering and Institute of Biomedical Engineering,
École Polytechnique de Montréal (EPM), Campus of the Université de Montréal, Montréal (Québec) Canada

*E-mail: sylvain.martel@polymtl.ca URL: www.nano.polymtl.ca

***Abstract*— MC-1 Magnetotactic Bacteria (MTB) are studied for their potential use as bio-carriers for drug delivery. The exploitation of the flagella combined with nanoparticles magnetite or magnetosomes chain embedded in each bacterium and used to change the swimming direction of each MTB through magnetotaxis provide both propulsion and steering in small diameters blood vessels. But for guiding these MTB towards a target, being capable to image these living bacteria *in vivo* using an existing medical imaging modality is essential. Here, it is shown that the magnetosomes embedded in each MTB can be used to track the displacement of these bacteria using an MRI system. In fact, these magnetosomes disturb the local magnetic field affecting T_1 and T_2-relaxation times during MRI. MR T_1-weitghted and T_2-weighted images as well as T_2-relaxivity of MTB are studied in order to validate the possibility of monitoring MTB drug delivery operations using a clinical MR scanner. This study proves that MTB affect much more the T_2-relaxation than T_1-relaxation rate and can be though as a negative contrast agent. The signal decay in the T_2-weighted images is found to change proportionally to the bacterial concentration. These results show that a bacterial concentration of 2.2×10^7 cells/mL can be detected using a T_2-weigthed image, which is very encouraging to further investigate the application of MTB for *in vivo* applications.**

***Index Terms*— Magnetic nanoparticles, Magnetic Resonance Imaging, bio-carriers, Magnetotactic bacteria.**

I. Introduction

One of the major *in vivo* applications where micro-carriers can play a significant role is cancer therapy. Modern oncology attempts to improve the efficacy of cancer treatments while reducing secondary toxicity. Many targeting strategies have been proposed, ranging from bioengineering approaches such as the use of liposome and micelle to the implementation of external guiding systems for magnetic nanoparticles and microbubbles [1,2]. These approaches show promising results but rely on a systemic injection and the transport of the anticancer agent through the blood flow. However, tumor microcirculation is characterized by tortuous vascular architectures, heterogeneous blood flows, leaky blood vessels and high interstitial pressure, leading to a poor delivery of therapeutic agents [3]. Therefore, the conception of a navigable microsystem that is self-propelled, small enough to pass through leaky vessels and capable to continue its route in the interstitial space to reach necrotic region of the tumor is of great importance.

Self-propelled biological microsystems such as bacteria are microorganisms that have proven their potential to reach deep tumor region and to proliferate in the tumor necrotic zone [4-6]. Following a systemic injection, some facultative or obligate anaerobic motile bacteria find in the microenvironment of the tumor, a privileged site for their proliferation. These bacteria are believed to reach tumor through chemotaxis towards substances produced by cancerous cells and to proliferate due to the poor oxygen level inside solid tumors. But in our knowledge, no external control has been applied until now to guide bacteria to the tumor. Hence, to allow control or guiding by an external computer, Magnetotactic Bacteria (MTB) are considered here.

II. Magnetic Control

MTB are flagellated microorganisms that can be controlled using an external magnetic field [7]. MTB synthesize intracellular Fe_3O_4 nanoparticles, called magnetosomes, assembled in a chain acting as a compass to influence through magnetotaxis [8,9] the swimming direction of the bacteria. The MTB cell sizes ranging between 1-3 µm in diameter gives them the ability to extravasate through the leaky tumor blood vessels with openings in the order of 4.7 µm [10].

A. Navigation Through Obstacles

MTB are very efficient to navigate in low Reynolds number hydrodynamics, and even if they keep following the applied magnetic field lines, they end up finding their way when an obstacle is reached. Fig.1 shows the way MTB reach a capillary entry when they hit a wall. First, we directed the MTB swarm to the upper right of the sample by magnetic navigation. Next, we inverted the magnetic field's direction causing the MTB to swim along the new direction until they hit a wall. Some bacteria gain access to the capillary entry as depicted in Fig. 1-c following a tumble motion as shown in Fig. 1-d after hitting the barrier.

B. Navigation Through Interstitial Space

A major problem that a drug encounters before reaching the cancerous cells is the high interstitial pressure of tumors [3].

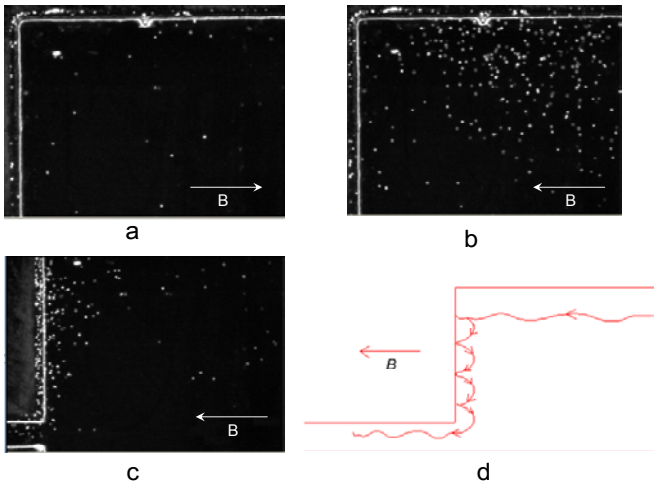

Fig. 1. Magnetotactic bacteria navigation in presence of an obstacle. (a) First of all, the bacteria swarm is directed to the upper right corner, (MTB are not shown because they are outside the FOV). (b) the magnetic field direction is inverted, and the MTB follow this new direction. (c) when the MTB hit a wall, they slide until they reach the capillary entry and continue their way. (d) Schematic view of the tumbling motion of the MTB when they hit an obstacle.

Bacteria can be very helpful in this circumstance since they have their own driven force. We have made a navigation test in a thin extracellular matrices which normally underlie cells *in vivo*. We used the BD Matrigel^{TM} basement membrane matrix (BD Biosciences, Two Oak Park, Bedford) in order to anticipate the motion of MTB in the interstitial space. We introduced in the sample fibers in the order of tens of micrometer in order to mimic the lymphatic vessels and the intracellular spacing as depicted in Fig. 2. The speed of MTB was significantly reduced because of the gel-like structure of the basement membrane. Still, MTB were able of small motion especially near the fiber where a fluid is supposed to form an interface with the basement membrane.

III. Magnetic Resonance Imaging

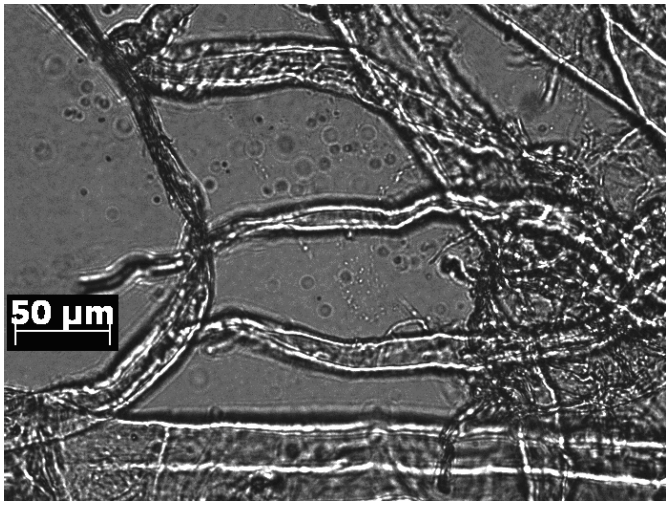

Fig. 2. Magnetotactic bacteria navigation in a basement membrane matrix. The speed of MTB was significantly reduced in this gel-like structure.

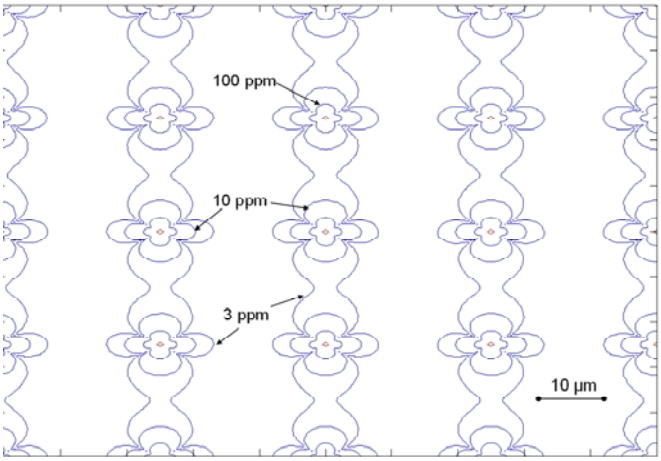

Fig. 3. Simulation of local magnetic field perturbation for a uniformly distributed concentration of MTB. The distance between MTB is taken to be 25 µm which corresponds to a concentration of approximately 10^7 bacteria/ml.

A. Magnetic Field Simulation

Superparamagnetic magnetite nanoparticles are often used as a contrast agent in Magnetic Resonance Imaging (MRI), particularly for cells labeling prior to MR-tracking [11]. In this case, nanoparticles are uniformly distributed and are attached to the cells via antibody binding. These nanoparticles alter the MR-signal because of their effect on the magnetic field. Simulation of the magnetic field of a uniformly distribution of MTB shows that the magnetosome chain will significantly disturb the local magnetic field. As depicted in Fig. 3, the field perturbation is significant near the bacteria with values greater than 100 ppm and decreasing further away from the bacterium. This is quite significant for our application considering that an accepted homogeneity level of modern MRI clinical scanner is approximately 5 ppm over a 50 cm diameter spherical volume at 1.5 T. On a macroscopic scale, these perturbations will cause geometric as well as intensity artifacts. On a microscopic scale however, these perturbations will affect the spin-lattice (T_1) and spin-spin (T_2) relaxation times. For this simulation, we consider a chain of 11 magnetosomes in length with a mean magnetosome diameter of 80 nm. The saturation magnetization of magnetite

Table 1: bacterial concentration and T_2-relaxation values for different MTB concentrations calculated from signal ratio measurements.

	Concentration $\times 10^7$ (bacteria/ml)	T2 (ms)
Sample 1 (medium)	0	646
Sample 2	2.2	305
Sample 3	3.5	203
Sample 4	4.8	172
Sample 5	6.2	156
Sample 6	6.7	114

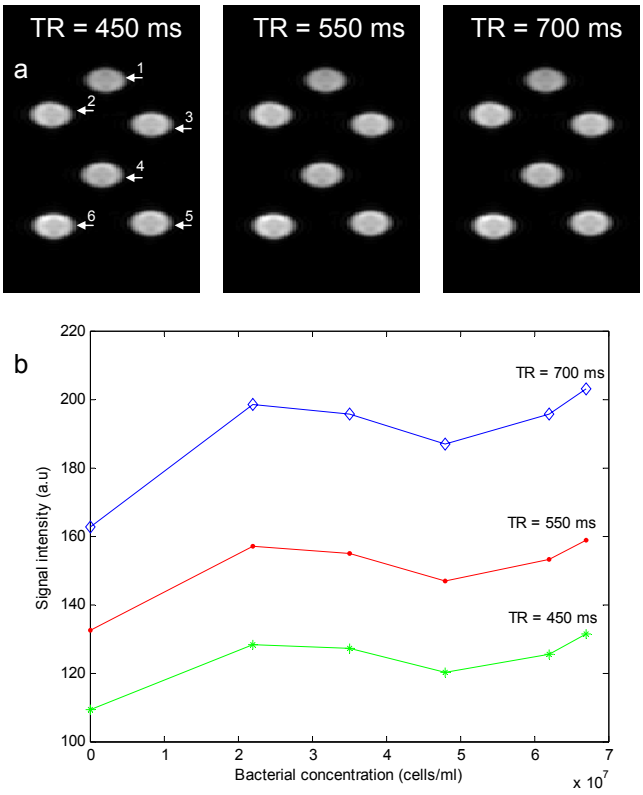

Fig. 4. T1 images of several concentration of magnetotactic bacteria (MTB) sample. Sample 1 to 6 (as numbered in a) show increasing concentrations starting from medium without MTB (sample 1). T1 weighted spin echo sequence with TE = 11 ms, three differents TR = 450/550/700 ms, a slice thickness of 20 mm, and a pixel spacing of 0.586 mm. (b) Signal intensity as a function of bacterial concentration for a T1-weighted acquisition with three different Repetition Time (TR) values. Notice that the signal contrast between samples of different concentrations is not important.

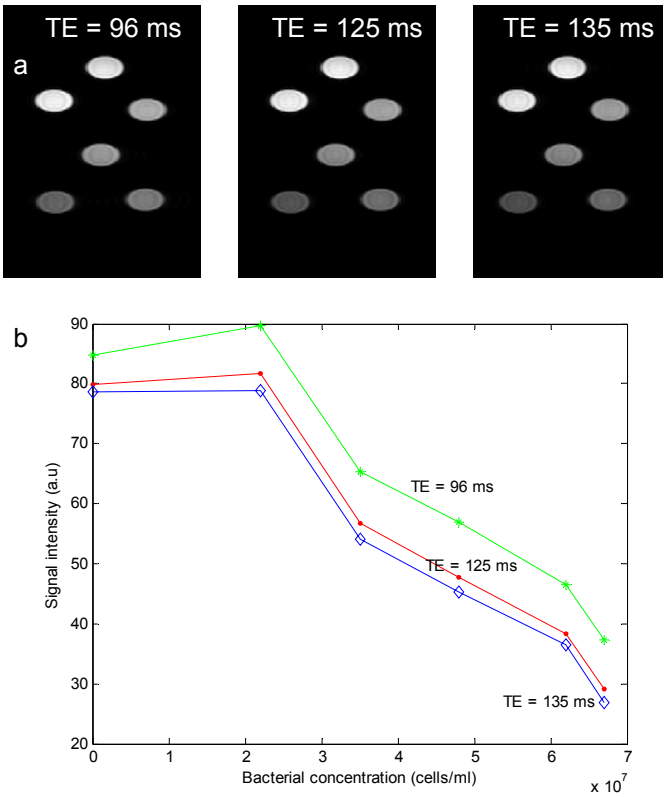

Fig. 5. T2 images of several concentration of magnetotactic bacteria (MTB) sample. Sample 1 to 6 (as numbered in a) show increasing concentrations starting from medium without MTB (sample 1). T2 weighted fast spin echo sequence with TR = 5096 ms, three differents TE = 96/125/135 ms, a slice thickness of 20 mm, and a pixel spacing of 0.293 mm. (b) Signal intensity as a function of bacterial concentration for a T2-weighted acquisition with three different Echo Time (TE) values. Notice that the signal contrast between samples of different bacterial concentrations is important.

is 0.6 Tesla.

B. Relaxation Time (T_1 and T_2) in Presence of MTB

In order to study the effect of MTB on the MR-Signal, several concentrations of MTB of MC-1 strain were prepared by centrifugation. Qualitative observation of bacterial motility and response to a magnetic field before and after concentrations though centrifugation was performed using a Zeiss Imager.Z1 microscope. Each concentration of the bacteria samples was determined by direct counting and by optical density measurements as presented in table 1. Each 1 ml MTB sample used for the experiments was inserted into a 2 ml Progene microtube. Images were run under a Siemens Avanto 1.5 T scanner using a wrist antenna. T_1-weighted spin echo sequence parameters were: TE = 11 ms with three different TR = 450/550/700 ms, slice thickness of 20 mm, and pixel spacing of 0.586 mm. T2 weighted fast spin echo sequence parameters were: TE = 96/125/135 ms, TR = 5096 ms and pixel spacing of 0.293 mm. Samples containing MTB show signal enhancement compared to the medium in T_1-weighted images as depicted in Fig. 4. However, this signal enhancement doesn't change much with higher MTB concentrations. The effect of the concentration of MTB is more evident on T_2-weighted images as depicted in Fig 5. As the concentration of bacteria increases, the signal decay becomes important. Table 1 presents T_2-relaxation values calculated from signal ratio measurement with different TE values. Fig. 6 shows the signal variation as a function of the

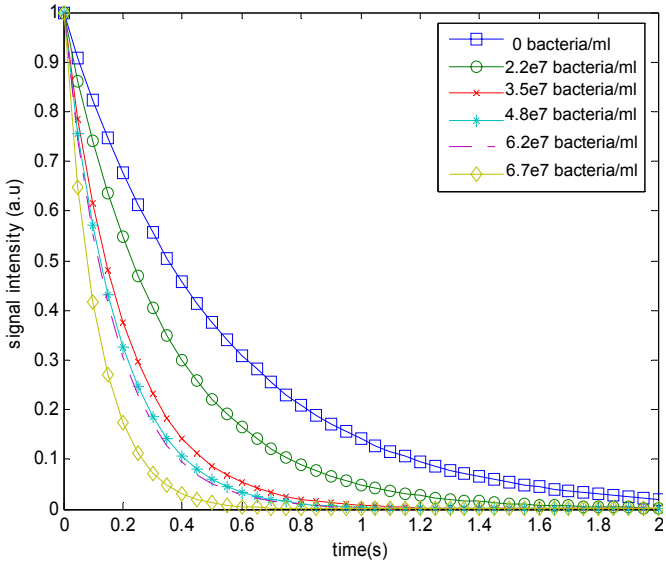

Fig. 6. T2 relaxation curves for different MTB concentrations as measured experimentally.

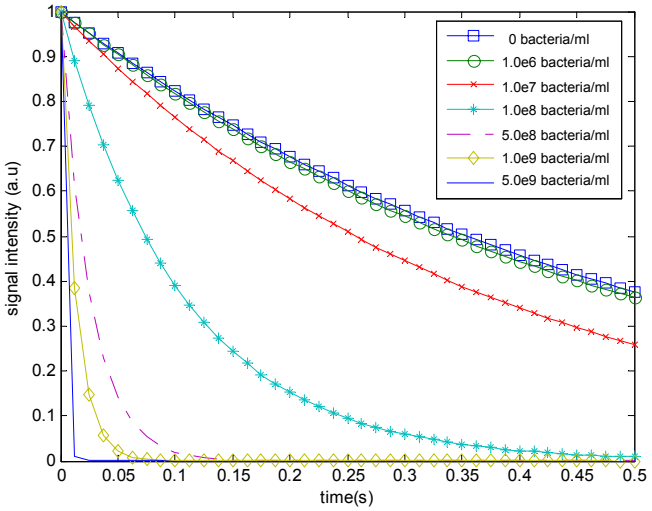

Fig. 7. T2 relaxation curves for different MTB concentrations simulated using the T_2-relaxivity value.

bacteria concentration for different TE values. As the TE value increases, the difference in signal between different concentrations becomes higher.

C. T_2-Relaxivity Measurement

We can calculate the T2-relaxivity for MTB, if the T2 value for a given concentration as well as for the medium is known. The relaxivity is related to the relaxation time and the concentration of the relaxing agent by:

$$\frac{1}{T_i} = \frac{1}{T_{i,0}} + \alpha_i [MTB], \quad i = 1,2 \tag{1}$$

where $T_{i,0}$ is the relaxation rate of the medium, $[MTB]$ is the concentration of the magnetotactic bacteria (cells/ml) and α_i is the relaxivity expressed in $(\frac{ml}{cells \cdot s})$ a property specific to the effect of MTB on the NMR signal. Equation 1 is generally used to characterize contrast agent in MRI [12]. The T_2-relaxivity value for MTB is found to be $\alpha_2 = 7.448 \cdot 10^{-8} (\frac{ml}{cells \cdot s})$. Once the relaxivity of an agent is known, the concentration of the MTB can be obtained on a voxel basis by direct measurement of the T2-relaxation value and inversion of equation 1. The T_2-relaxation curve as approximated by the relaxivity value is shown for several MTB concentrations in Fig. 7. Notice that at a bacterial concentration lower than 10^6 bacteria/ml, no contrast will result compared to the background. However, for higher concentrations a contrast can be obtained until the signal completely disappear from MTB solution where the concentration is in the order of $5 \cdot 10^9$ bacteria/ml. Previous studies on bacterial analysis and quantification under MRI have reported the possibility to detect concentrations on the order of 10^8-10^9 cells/mL of magnetically labeled bacteria [11].

IV. Conclusion

Bacterial tumor targeting has gained renewed interest these last years because of the ability of some bacteria to reach deep tumor region and induce a therapeutic effect. However, we propose a new mechanism of drug delivery using magnetically controllable bacteria. We show the magnetic control in different settings and the MRI characteristics of different bacterial concentration solutions. Future works will be directed toward closing the loop of the magnetic control and MRI tracking in order to be able to navigate MTB through complex pathways and *in vivo* in real-time.

Acknowledgment

This project is supported in part by a Canada Research Chair (CRC) in Micro/Nanosystem Development, Fabrication and Validation, the Canada Foundation for Innovation (CFI), the National Sciences and Engineering Research Council of Canada (NSERC), and the Fonds Québécois de Recherche sur la Nature et les Technologies (FQRNT).

References

[1] E. S. Kawasaki, A. Player, "Nanotechnology, nanomedicine, and the development of new, effective therapies for cancer," Nanomedicine, I, 101-109, 2005.

[2] J. K. Vasir, M. K Reddy, V. Labhasetwar, "Nanosystems in Drug Targeting: Opportunities and Challenges," Current Nanoscience, 1(1), 45-62, 2005.

[3] R.K. Jain. "Delivery of Molecular and Cellular Medicine to Solid Tumors," Adv. Drug Deliv. Rev., 46: 149-168, 2001.

[4] N. S. Forbes, L. L. Munn, D. Fukumura and R. K. Jain, "Sparse initial entrapment of systemically injected salmonella typhimurium leads to heterogeneous accumulation within tumor necrosis, " Cancer Research 63:5188-5193, 2003.

[5] R. W. Kasinskas, N. S. Forbes, "Salmonella typhimurium specifically chemotax and proliferate in heterogeneous tumor tissue in vitro," Biotechnology and Bioengineering, 94(4), p 710-721, 2006.

[6] C. Bettegowda, L. H. Dang, R. Abrams, and al., "Overcoming the hypoxic barrier to radiation therapy with anaerobic bacteria, " Proc Natl Acad Sci, 100(25),15083–15088, 2003.

[7] S. Martel, C. Tremblay, S. Ngakeng, and G. Langlois, "Controlled manipulation and actuation of micro-objects with magnetotactic bacteria," Applied Physics Letters, 89, 233804-233806, 2006.

[8] R. P. Blakemore, "Magnetotactic bacteria [in geomagnetic field]," Science, 190, 377-379, 1975.

[9] R. B. Frankel, D. A. Bazylinski, M. S. Johnson, B. L. Taylor, "Magneto-aerotaxis in marine coccoid bacteria," Biophysics Journal, 73, 994-1000, 1997.

[10] H. Hashizume, P. Baluk, S. Morikawa, J.W. McLean, G. Thurston, S. Roberge, R.K. Jain and D.M. McDonald, "Openings Between Defective Endothelial Cells Contribute to Tumor Vessel Leakiness," American Journal of Pathology, 156: 1363-1380, 2000.

[11] M.S. Olson, R. M. Ford, J. A. Smith, E. J. Fernandez, "Analysis of column tortuosity for MnCl2 and bacterial diffusion using magnetic resonance imaging," Environmental Science and Technology, 39(1), 149-154, 2005.

[12] E. Toth, L. Helm, A. E. Merbach, "Relaxivity of MRI contrast agents," Topics in Current Chemistry, 221, 61-101, 2002.